

Infrared Machine Vision for Detection and Characterization of Defects Present in a Mild Steel Material

Pranav Yogesh Mahajan¹, Aneesh Bajwa¹, Keshav¹, Nandani Bansal¹, Geetika Dua^{1a}, Amanpreet Kaur¹, Vanita Arora²

¹Thapar Institute of Engineering and Technology, Patiala.147004

²Indian Institute of Information Technology Una, Vill. Saloh, Teh. Haroli, Distt. Una Himachal Pradesh, India-177209.

^aEmail: geetikadua09@gmail.com

Abstract

Significant advancements in machine vision and thermal imaging have provided an advantage in non-destructive testing and evaluating different materials. This work presents an approach to combining thermal wave imaging with machine vision for a fast, accurate way to detect and characterize the sub-surface defects and their features present in a solid material. Machine vision-based defect detection approaches attract the research community due to their reliable performance in employing the stimulated thermal response in active thermal wave imaging. A thermal source stimulates the material surface while the infrared camera captures its thermal response, extracts features from the thermal pattern, and feeds them into a machine vision-based algorithm for characterization. This proposed method improves the detectability reliability regarding qualified characteristics of defects.

Keywords: *MachineVision; Non-destructive testing; Scale-invariant feature transform, Watershed transform*

1.Introduction

Infrared thermography (IRT) has emerged widely as a method for non-destructive testing as it offers non-contact, comprehensive area detection of material defects. The principle of infrared thermography is based on the physical phenomenon that any object of a temperature above absolute zero emits electromagnetic radiation. The infrared camera further covers the emitted radiation into temperature and displays the images showing thermal variations [1-6].

Infrared thermography is further classified as passive thermography and active thermography. In passive thermography, without any external known source, a natural thermal response on the test material surface is used to identify subsurface defects. An external heat source stimulates the test sample in active thermography, and the corresponding thermal response is recorded using an infrared camera. Various processing methods can do further subsurface defect detection.

Depending on the external stimulus, the active thermography is classified as Pulsed thermography (PT) [2-3], Pulse phased thermography (PPT) [4-5], Lock-in thermography (LT) [6-7], and other aperiodic thermal wave imaging methods like Frequency Modulated Thermal Wave Imaging (FMTWI) [8-9]. In Pulsed thermography (PT), the surface of the test material is energized using a high peak power source within a short duration of time, and the corresponding thermal response is collected from the surface of the test material. Because of the high peak power and short duration of time, the total test sample cannot absorb heat uniformly and enters two problems non-uniform emissivity and non-uniform radiation. In lock-in thermography (LT), instead of high peak power, a mono-frequency continuous wave is used as an external stimulus, and the infrared camera captures the corresponding thermal response. The thermal response collected from the infrared camera is analyzed using phase-based analysis, which is less sensitive to non-uniform radiation and non-uniform emissivity. Because of mono frequency, repetition of the

experiment is needed to detect the defects at various depths.

Pulse-phase thermography (PPT) combines pulse and lock-in thermography, like pulse energy for stimulation and phase-based analysis for defect detection. This experimentation is like pulse thermography, but Fourier Transform carries analysis applied over thermal response to extract the phase delay. Frequency modulated thermal wave imaging.

(FMTWI) [8-12] is introduced to overcome the above problems. This method imposed a suitable band of frequencies over the test sample within single experimentation. Frequency modulated thermal wave imaging, where the heating waveform phase relations are adjusted over bandwidth in such a way that chirps (frequency modulated) signal, with much-reduced peak power, is produced. FMTWI, while retaining all characteristics of lock-in thermography, has the added advantage of overcoming the blind frequency problem. The captured thermograms are further processed using matched filtering (pulse compression) [12-16].

The main objective of this paper is to propose a method to detect and classify defects in solid materials. This work presents an approach combining thermal wave imaging with machine vision for a fast, accurate way to detect and classify the sub-surface defects and their features in a mild steel material. A machine vision-based discrimination modality has been proposed for an aperiodic analysis to be used for sub-surface characterization. This proposed modality improves testability and reliability presents the best detection in terms of quantified characteristics of the defects.

Machine-vision algorithms provide us with valuable information about the defects present [17-20]. Various signal and image processing schemes are generally applied to observed thermal response to validate defect detection, depth quantification, and material property estimation [20]. However, in the present scenario where artificial intelligence and machine learning are ruling the world, these signal processing and manual inspection-based modalities also lag the performance, quality, and time. Machine vision techniques are utilized to overcome such cases and be synchronized with the present world scenario to detect and characterize the defects placed in materials.

In this paper, machine learning techniques like Scale-invariant feature transform (SIFT) is employed on pre-processed thermal response acquired from numerically simulated mild steel sample with various types of

defects placed at different depths. The sample is excited by frequency-modulated heat flux. Further, the watershed transform-based region-based segmentation approach is employed for localizing the defects accurately.

2. Modeling and simulation

In this work, a 3D Finite element analysis (FEA) has been carried out on a steel sample using COMSOL Multiphysics. This software simulates designs, devices, and processes in all engineering, manufacturing, and scientific research fields [21-22]. COMSOL Multiphysics is a simulation platform that provides fully coupled multiphysics and single-physics modeling capabilities. The Model Builder includes all of the steps in the modeling workflow, from defining geometries, material properties, and the physics that describe specific phenomena to solving and post-processing models for producing accurate results. The two mild steel sample (one training and the other testing) models with eighteen defects, six each of three different material, air, water, and oil (shown in Fig.1), has been modeled with a finer mesh using 3D tetrahedral elements.

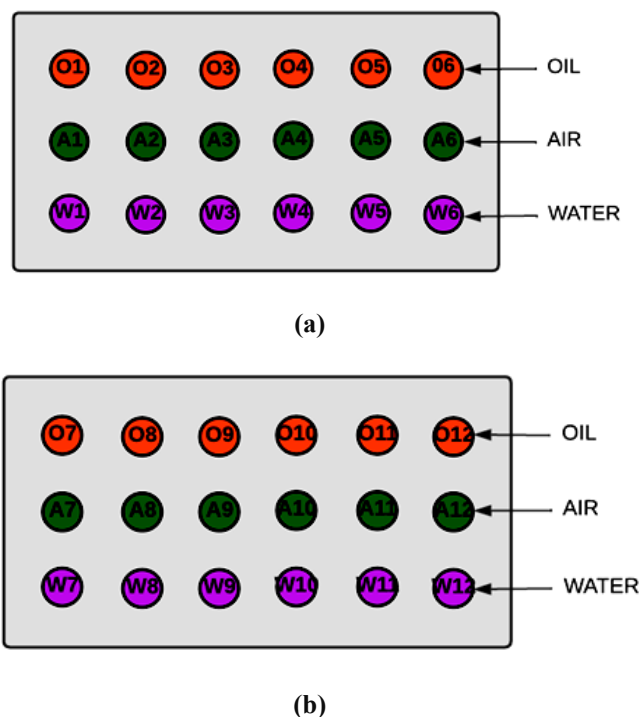


Fig.1 Layout of the modeled mild steel sample with inclusions. (a) Training sample (b). Testing sample

The defects are further placed at different depths having the same diameter (20 mm). The defect's depths are shown in Table 1. The FEA is carried out by

imposing an LFM heat flux (with frequency varying from 0.01 Hz to 0.1 Hz for 100 s) over the surface of the test material, and the infrared camera captures the resultant surface thermal response at a frequency of 25 Hz. The simulations are carried out under adiabatic boundary conditions, with the sample at an ambient temperature of 300 K.

Table.1 Depths of different defects

S.No. (Oil (o), Air(a), Water (w))	Depth (mm)	S.No. (Oil, Air, Water)	Depth (mm)
1	1	7	0.8
2	1.4	8	1.2
3	1.8	9	1.6
4	2.2	10	2
5	2.6	11	2.4
6	3	12	2.8

The thermal properties of the materials used are as given in Table 2.

Table 2. Thermal properties

Material	Density (ρ) (Kg/m ³)	Thermal Conductivity (k) W/(m*K))	Specific Heat (c) (J/(Kg*K))
Air	1.23	0.025	1007
Water	1000	0.5576	4200
Oil	1510	0.162	749
Mild Steel	7850	60.5	434

The simulated data is further processed using signal processing and machine vision based algorithms as described in the next section.

3. Post processing methods

3.1 Polynomial Fitting

The recorded thermal response is first processed to obtain a zero mean thermal response using an appropriate polynomial fit. Using this method, we model or represent a data spread by assigning the best fit function (curve) along the entire range [8-10, 23].

3.2 Pulse Compression

Pulse compression is a statistical technique for determining how one variable changes with the other variable. It gives us an idea of the relationship between the two variables. It is a bi-variate analysis measure that describes the association between different variables. We used correlation to find how the size of the defect varies in the thermal image when the depth radius of the defect is varied and tried to develop a relationship between them. After finding a relationship between these parameters, it became easier to train and tests the machine vision-based model [12-15,17].

3.3 Watershed Transform

The watershed transformation can be classified as a region-based segmentation approach. The intuitive idea underlying this method comes from geography. Watershed algorithms are used in image processing primarily for object segmentation, that is, for separating different objects in an image. The algorithm allows for counting the number of defects or for further analysis of the separated object [24].

3.4 SIFT

Scale-invariant feature transform (SIFT) is a machine-vision algorithm to detect, describe, and match local features in images (thermograms). Interesting points can be extracted for any object in an image to provide a “feature description” of the object. This description, extracted from a training image, can then be used to identify the object when attempting to locate the object in a test image containing many other objects. To perform reliable recognition, extracting features from the training image to be detectable even under changes in image scale, noise, and illumination is essential. Such points usually lie on high-contrast regions of the image, such as object edges [18, 24-27].

In this work, SIFT is first applied, determining a few best frames from the 4999 frames (pulse-compressed thermograms) dataset. Then, the best frame is determined using this technique.

4. Results and discussions

The present works highlight the capability of the proposed approach in detecting and characterizing defects present in a structural mild steel sample. In this approach, the test material can undergo a known controlled frequency modulated thermal stimulation sweeping their entire frequency range from 0.01Hz to 0.1 Hz in 100 s, and the infrared camera captures the corresponding thermal response over the surface.

Additive white Gaussian noise with a signal-to-noise ratio being 30 dB is added to the obtained thermal response for the imposed incident heat flux. Noise is artificially added to test the capability of the proposed approach to detect the subsurface density variations. The temporal mean raise from the noisy thermal response is removed using an appropriate polynomial fit. Fig.2. shows the corresponding mean-zero thermograms for the training and testing modeled samples.

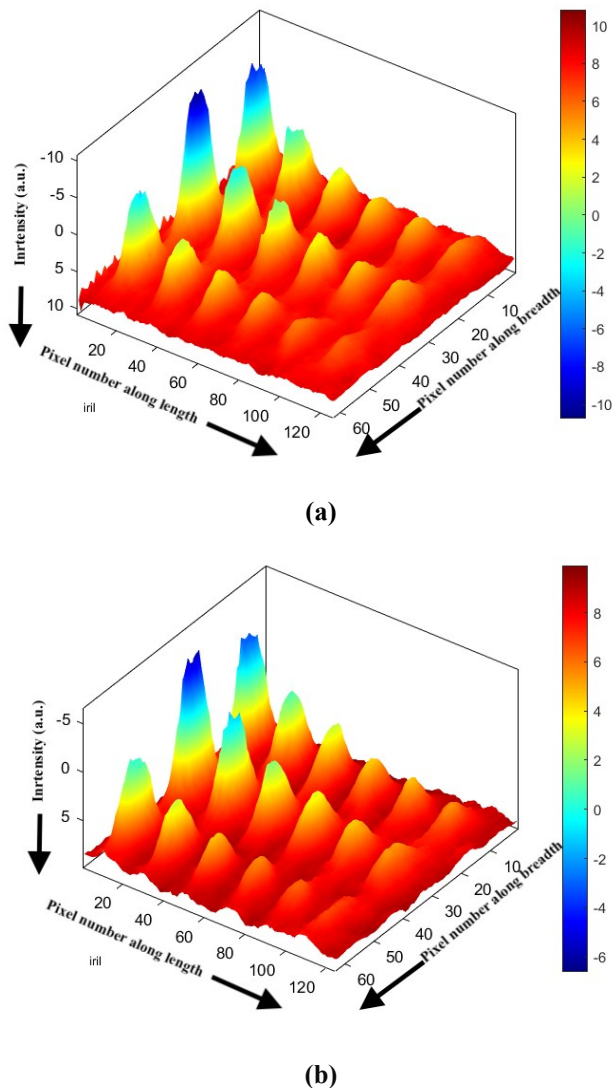


Fig.2 Zero mean thermograms. (a) Training sample (b). Testing sample

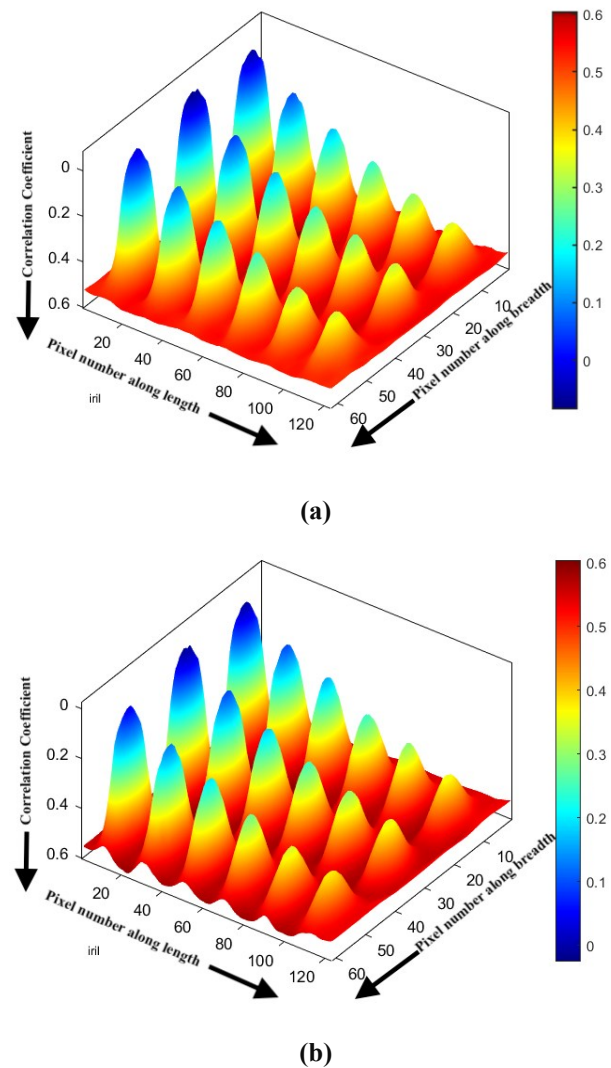


Fig.3 Pulse-compressed thermograms. (a) Training sample (b). Testing sample

As shown in this section, the aforementioned signal processing, and machine vision-based techniques are further applied to mean zero data and results. Pulse compression analysis is performed on the mean zero data for the training and testing sample data. The resulting thermograms are obtained, and the best frame is selected using SIFT algorithm. It is obtained at 1.5 s.

Fig.3. shows the pulse-compressed thermograms.

Further, applying the watershed algorithm to the chosen best frame provides the segmented thermogram. The algorithm also determines the count of the defects present in the sample. The resulting thermograms are as shown in Fig.4.

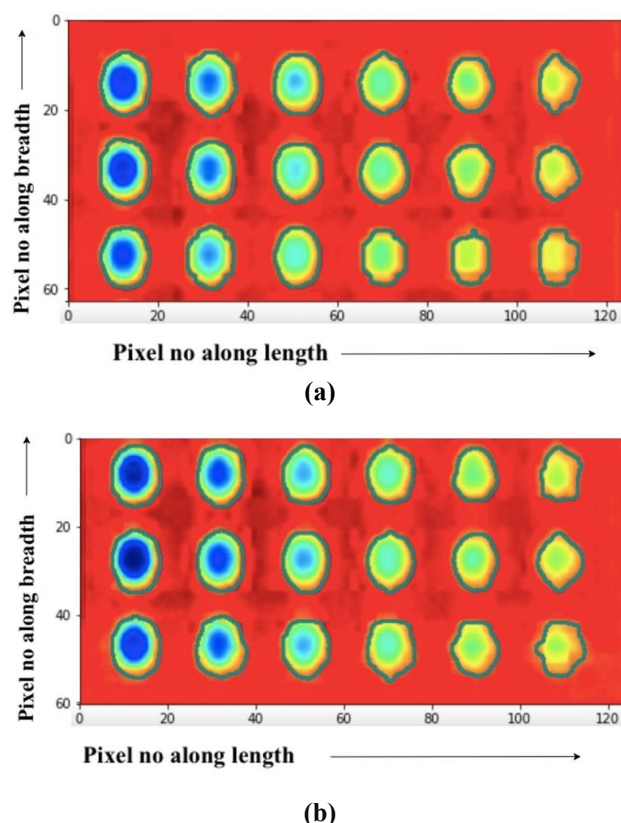


Fig.4 Segmented thermograms. (a) Training sample (b). Testing sample

Furthermore, pulse compression results are used to determine the type of material (air, water, or oil). The relationship between correlation peak shifts and depths of defects present, a set of pixels (3x3 region around the center of each defect) are chosen, and their correlation coefficient is calculated with that of chosen reference pixel.

Peak shifts are determined for the peak of auto-correlation of reference pixels. Moreover, a relationship between depths and these peak shifts is constructed.

This process is repeated for defects containing different materials: air, water, and oil. The results show the maximum variation in defects with air and defects with water has the minimum, which is true as water has the highest thermal effusivity and air has the lowest. The results are verified for the training sample and plotted as shown in the bar diagram in Fig.5.

5. Conclusions

The present manuscript demonstrates the capability of Frequency modulated infrared thermographic technique combined with the machine vision algorithms. This infrared machine vision technology provides the accurate detection and characterization of the defects.

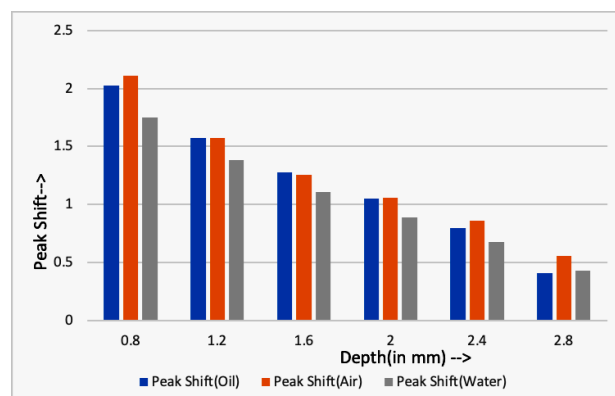


Fig.5 Variation of Peak shifts with Depth for three different materials

FMTWI technique is applied on a mild steel sample with defects of different types and placed at different depths. Pulse-compressed thermogram obtained from post-processing is considered as input to the machine vision algorithms. Further, defects characterization is done to determine the relationship between a different material's peak shift and depth. The relation obtained can also be used in the future to determine the depths of the defect. The count of defects has been calculated using the watershed algorithm.

6. References

- [1] X. P. V. Maldague (2001), "Theory and Practice of Infrared Thermography for Non- Destructive Testing," John Wiley & Sons Inc.
- [2] D. P. Almond and S. K. Lau (1994), "Defect sizing by transient thermography I: An analytical treatment," *Journal of Physics D: Applied Physics*, 27 (5), pp. 1063-1069.
- [3] D. L. Balageas, J.C. Krapez, P. Cielo (1986), "Pulsed photothermal modeling of layered materials," *Journal of Applied Physics*, 59 (2), pp. 348-357.
- [4] X. Maldague and S. Marinetti (2003), "Pulse Phase Infrared Thermography," *Review of Scientific Instruments*, 74 (1 II), pp. 417-419.
- [5] X. Maldague and S. Marinetti (1996), "Pulse phase infrared thermography," *Journal of applied physics*, vol. 79, no. 5, pp. 2694-2698.
- [6] G. Busse (1979), "Optoacoustic phase angle measurement for probing a metal," *Applied Physics Letters*, 35 (10), pp. 759-760.
- [7] G. Busse, D. Wu, W. Karpen, "Thermal wave imaging with phase-sensitive modulated thermography," *Journal of Applied Physics*, 71 (8), pp. 3962-3965, 1992.

-
- [8] R. Mulaveesala and S. Tuli (2006), "Theory of frequency modulated thermal wave imaging for nondestructive subsurface defect detection," *Applied Physics Letters*, 89 (19), art.no. 91913.
- [9] S. Tuli and R. Mulaveesala, "Defect detection by pulse compression in frequency modulated thermal wave imaging," *Quantitative InfraRed Thermography Journal*, vol. 2(1), pp. 41-54, 2005.
- [10] Ghali V S and Mulaveesala R 2010 Frequency modulated thermal wave imaging techniques for non-destructive testing, *Insight: Non-Destructive Testing and Condition Monitoring* 52, 475-480
- [11] Arora V, Mulaveesala R and Bison P 2016 Effect of Spectral Reshaping on Frequency Modulated Thermal Wave Imaging for Non-destructive Testing and Evaluation of Steel Material, *Journal of Nondestructive Evaluation* 35, 1-7.
- [12] Kaur K and Mulaveesala R (2019), "An efficient data processing approach for frequency modulated thermal wave imaging for inspection of steel material", *Infrared Physics and Technology*, 103, 103083.
- [13] Dua G, Arora V and Mulaveesala R (2021), "Defect Detection Capabilities of Pulse Compression Based Infrared Non-Destructive Testing and Evaluation", *IEEE Sensors Journal* 21, 7940-7947.
- [14] Arora V, Mulaveesala R, Rani A, Kumar S, Kher V, Mishra P, Kaur J, Dua G and Jha R (2021), "Infrared Image Correlation for Non-destructive Testing and Evaluation of Materials", *Journal of Nondestructive Evaluation*, 40, 1-7.
- [15] Mulaveesala R, Arora V and Dua G (2021), "Pulse Compression Favorable Thermal Wave Imaging Techniques for Non-Destructive Testing and Evaluation of Materials", *IEEE Sensors Journal*, 21, 12789-12797.
- [16] Kaur K and Mulaveesala R (2019), "Experimental investigation on noise rejection capabilities of pulse compression favourable frequency-modulated thermal wave imaging", *Electronics Letters*, 55, 352-353.
- [17] Duan Y, Liu S, Hu C, Hu J, Zhang H, Yan Y, Tao N, Zhang C, Maldague X and Fang Q (2019), "Automated defect classification in infrared thermography based on a neural network", *NDT & E International* 107, 102147.
- [18] Hossein-Nejad Z, Agahi H, and Mahmoodzadeh A (2020), "Detailed review of the scale invariant feature transform (sift) algorithm; concepts, indices and applications", *Journal of Machine Vision and Image Processing*, 7(1), 165-190.
- [19] Dudek G, Dudzik S 2018 Classification Tree for Material Defect Detection Using Active Thermography, *Advances in Intelligent Systems and Computing*, 655, 118-127
- [20] Fang Q, Nguyen B D, Castanedo C I, Duan Y and Maldague II X (2020), "Automatic defect detection in infrared thermography by deep learning algorithm", *Thermosense: thermal infrared applications XLII SPIE* pp 180-195.
- [21] Mulaveesala R and Dua G (2016), "Non-invasive and non-ionizing depth resolved infra-red imaging for detection and evaluation of breast cancer: A numerical study", *Biomedical Physics and Engineering Express*, 2, 055004.
- [22] Arora V, Mulaveesala R, Dua G and Sharma A (2020), "Thermal non-destructive testing and evaluation for subsurface slag detection: Numerical modeling", *Insight: Non-Destructive Testing and Condition Monitoring*, 62, 264-268.
- [23] Cardone, Daniela, Edoardo Spadolini, David Perpetuini, Chiara Filippini, Antonio Maria Chiarelli, and Arcangelo Merla (2021), "Automated warping procedure for facial thermal imaging based on features identification in the visible domain", *Infrared Physics & Technology*, 112, 103595.
- [24] Gamarra, Margarita, Eduardo Zurek, Hugo Jair Escalante, Leidy Hurtado, and Homero San-Juan-Vergara (2019), "Split and merge watershed: A two-step method for cell segmentation in fluorescence microscopy images, *Biomedical signal processing and control*, 53, 101575.
- [25] Mery D, da Silva R R, Calôba L P and Rebello J M (2003), "Pattern recognition in the automatic inspection of aluminium castings", *Insight-Non-Destructive Testing and Condition Monitoring*, 45, 475-483.
- [26] Li, Henan, Shigang Wang, Yan Zhao, Jian Wei, and Meilan Piao (2021), "Large-scale elemental image array generation in integral imaging based on scale invariant feature transform and discrete viewpoint acquisition", *Displays*, 69, 102025.
- [27] Jubair, Aliaa S., Aliaa Jaber Mahna, and H. I. Wahhab (2019), "Scale invariant feature transform based method for objects matching", *International Russian Automation Conference (RusAutoCon)*, pp. 1-5.
-